RESEARCH ARTICLE

Proteomic profiling identifies the SIM-associated complex of KSHV-encoded LANA

Jin Gan[1], Chong Wang[1]*, Yanling Jin[2]*, Yi Guo[3]*, Feng Xu[4], Qing Zhu[1], Ling Ding[1], Hong Shang[3], Junwen Wang[4], Fang Wei[2]**, Qiliang Cai[1] and Erle S. Robertson[5]***

[1] MOE& MOH Key Laboratory of Medical Molecular Virology, School of Basic Medicine, Shanghai Medical College, Fudan University, Shanghai, P. R. China
[2] ShengYushou Center of Cell Biology and Immunology, School of Life Sciences and Biotechnology, Shanghai Jiao Tong University, Shanghai, P. R. China
[3] Department of Gynecology, Key laboratory of AIDS immunology of Ministry of Health, First Affiliated Hospital of China Medical University, Shenyang, P. R. China
[4] Department of Biochemistry and Center for Genome Science, The University of Hong Kong, Hong Kong, P. R. China
[5] Department of Microbiology and Abramson Comprehensive Cancer Center, Perelman School of Medicine at the University of Pennsylvania, Philadelphia, PA, USA

Received: December 26, 2014
Revised: February 11, 2015
Accepted: April 17, 2015

The Kaposi's sarcoma-associated herpesvirus (KSHV) encoded latent nuclear antigen latency-associated nuclear antigen (LANA) plays an essential role in viral episome maintenance. LANA also contributes to DNA replication and tumorigenesis during latency. Recent studies suggested that LANA was involved in regulation of SUMOylation, which results in chromatin silencing. To examine the pleiotropic effects of LANA protein on host cell gene expression, we utilized MS analysis to identify cellular proteins associated with the small ubiquitin related modifier (SUMO) interacting motif of LANA ($LANA^{SIM}$). In addition to the six bands identified as substantially associated with $LANA^{SIM}$, 151 proteins were positively identified by MS/MS analysis. Compared with previous proteomic analysis of the N- and C-truncated mutants of LANA ($LANA^{NC}$), our results revealed that a complex of specific proteins with relatively high SUMOylation and SIM motifs is associated with $LANA^{SIM}$. Intriguingly, consistent with our previous report that identified KAP1 as a key component, the in vitro SUMO-2-modified isoform has a substantially higher affinity with $LANA^{SIM}$ than the SUMO-1-modified isoform. Moreover, via cluster and pathway analysis, we proposed a hypothetical model for the $LANA^{SIM}$ regulatory circuit involving aberrant SUMOylation of cell cycle (particular mitotic), DNA unwinding and replication, and pre-mRNA/mRNA processing related proteins. This study provides a SUMOylated and non-SUMOylated proteome profile of $LANA^{SIM}$-associated complex and facilitates our understanding that viral-mediated gene regulation through SUMOylation is important for Kaposi's sarcoma-associated herpesvirus persistence and pathogenesis.

Keywords:
KSHV / LANA / Microbiology / SUMO-interacting motif

1 Introduction

PTM with the small ubiquitin related modifier (SUMO) is one of the key strategies for protein regulation in eukaryotic

Correspondence: Qiliang Cai, MOE & MOH Key Laboratory of Medical Molecular Virology, School of Basic Medicine, Shanghai Medical College, Fudan University, Shanghai 200032, P. R. China
E-mail: qiliang@fudan.edu.cn

Abbreviations: KSHV, Kaposi's sarcoma-associated herpesvirus; **LANA**, latency-associated nuclear antigen; **NE**, nuclear extract; **SIM**, SUMO-interacting motif; **SUMO**, small ubiquitin related modifier

*These authors contributed equally to this work.
**Additional corresponding author: Professor Fang Wei,
E-mail: fangwei@sjtu.edu.cn; Dr. Erle S. Robertson,
E-mail: erle@upenn.edu

Colour Online: See the article online to view Figs. 1–4 in colour.

cells. It is essential for a wide range of cellular processes including chromatin organization, transcription, DNA repair, subcellular localization, protein stability, and signal transduction [1, 2]. However, the aberrance of SUMO regulation is highly associated with various diseases and cancers [1, 3]. In vertebrate cells, there are at least four isoforms of SUMO are identified—SUMO-1, SUMO-2, SUMO-3, and SUMO-4. SUMO-2 and SUMO-3 collectively are referred to as SUMO-2/3, due to their shared 97% sequence identity, and are 50% identical with SUMO-1 [4]. SUMO-1, -2, and -3 are ubiquitous in human cells, while SUMO-4 is tissue specific and its biological functions remain unclear [4, 5]. Covalent and reversible attachment of SUMO to a target protein requires the E1 heterodimeric SUMO-activating enzyme Uba2-Aos1 and the E2 SUMO-conjugating enzyme Ubc9 [4]. Although many substrates can be SUMOylated directly by Ubc9 in vitro, it is believed that in vivo the specificity of the reaction is regulated by SUMO E3 ligases, which stimulate the transfer of SUMO from Ubc9 to a lysine chain in the substrate molecule [6]. To date, a core consensus motif φKxE has been identified as SUMOylation sites, in which φ presents a large hydrophobic amino acid, K is the SUMOylation site, X indicates any amino acid, and E is glutamic acid [7]. A major difference between SUMO-1 and SUMO-2/3 is that SUMO-2/3 can form poly-SUMO chains on substrate proteins through their internal φKxE motif [7]. However, the collective experimental data show that approximately 40% of known SUMOylation sites do not conform to this canonical consensus motif, while an algorithm using a group-based prediction system reveals noncanonical SUMOylation sites [8, 9]. In addition to covalent modification by SUMO, proteins may also interact noncovalently with SUMO through their SUMO-interacting motifs (SIMs), which are usually characterized by a stretch of consensus hydrophobic residues (i.e. -V/I-x-V/I-V/I-) [10, 11]. The function of these motifs enables interactions between a SUMOylated protein and its partner. Since the discovery of SIMs and their roles in regulating the activities of cellular proteins, substantial studies on noncovalent interactions between viral proteins and cellular SUMO family members have been reported [3, 12].

Kaposi's sarcoma-associated herpesvirus (KSHV, also known as human herpesvirus 8), the second identified oncogenic DNA virus, has been linked to several human malignancies including Kaposi's sarcoma, primary effusion lymphoma, and multicentric Castleman's disease [13, 14]. Like other herpesvirus, KSHV has latent and lytic replication life cycle, which is tightly regulated by its own genes. One of which, the latency-associated nuclear antigen (LANA) encoded by ORF73, is the dominant molecule essential for establishment and maintenance of KSHV latent infection and pathogenesis [15–17]. LANA is a multifunctional protein involved in regulation of cellular and viral gene transcription, DNA replication, and tethering the viral episomal DNA to the host chromosomes during mitosis [18]. The molecular mechanisms of how LANA performs the range of functions are actively investigated. In addition to the accumulating body of research on the biological functions of LANA, we and others recently revealed that LANA was SUMOylated and contains unique SIM motifs, which is essential for KSHV persistence during latency [11, 19]. Therefore, the SUMO pathway may play a key role in LANA-mediated regulation of the KSHV life cycle and a variety of host cellular processes.

In this study, to further obtain a more comprehensive view of the role of the SIM motif of LANA ($LANA^{SIM}$) in KSHV latency, we explored the profile of cellular proteins associated with $LANA^{SIM}$ through proteomic studies, and addressed the difference of SUMOylated and non-SUMOylated proteomic interactions between the $LANA^{SIM}$ and $LANA^{NC}$ (the N- and C-truncated mutants of LANA) residues [20], and highlighted the regulatory functions of $LANA^{SIM}$ associated with the cellular signal pathways. These results provide new insights into the range of mechanisms linked to LANA functions in regulating KSHV persistence and pathogenesis at a molecule network level.

2 Materials and methods

2.1 Preparation of nuclear extracts

To harvest nuclear extracts (NEs), cells were resuspended in four times the volume of the pellet in NE buffer A (10 mM HEPES pH 7.9, 10 mM KCl, 1.5 mM $MgCl_2$ with protease inhibitors) after cold PBS wash, incubated on ice for 1 h, and then transferred to a prechilled douncer followed by homogenization with 25 strokes. Homogenized samples were transferred to Eppendorf tubes and spun at 2000 rpm for 5 min at 4°C. The supernatant was aspirated and the pellet resuspended in two times the volume of NE Buffer B (20 mM HEPES pH 7.9, 10% glycerol, 420 mM NaCl, 1.5 mM $MgCl_2$, 0.2 mM EDTA with protease inhibitors). This was incubated on ice for 30 min and centrifuged at 13 000 rpm for 20 min at 4°C. The supernatants were transferred to fresh Eppendorf tubes and an equal volume of NE Buffer C (20 mM HEPES pH 7.9, 30% glycerol, 1.5 mM $MgCl_2$, 0.2 mM EDTA with protease inhibitors) added. This was then aliquoted and the samples snap frozen at –80°C before use.

2.2 Protein expression and in vitro pull-down assays

Overnight starter cultures (50 mL) of BL21 (DE3) transformed with plasmid expressing GST or GST-fused protein were used to individually inoculated 500 mL of Luria broth culture medium with specific antibiotic and grown at 30°C to a density of appropriately 0.6 optical density at 600 nm. After 1 mM IPTG induction at 30°C for 4 h, the bacteria were collected and sonicated in lysis buffer (20 mM Tris–HCl pH 8.0, 100 mM NaCl, 0.5% NP40, 1 mM EDTA, 1 M DTT, 5% Sarkosyl, and the protease inhibitor cocktail). Recombinant proteins GST, GST-SIM (240-300 of LANA), GST-$LANA_{1\text{-}329}$, or GST-$LANA_{1\text{-}329}\Delta$SIM were purified by glutathione sepharose chromatography according to manufacturer's instruction

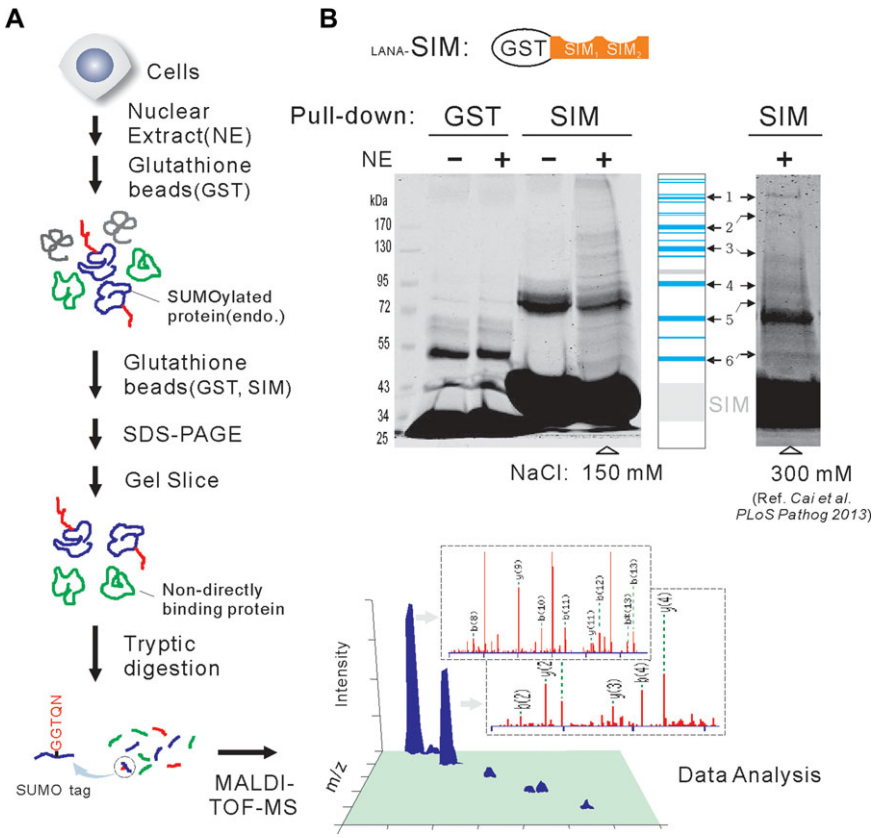

Figure 1. Overview of strategy to identify LANA^{SIM}-associated peptides from protein extracts of human cells. (A) Streamlined workflow for identification of proteomes. Total proteins of nuclear extract from primary effusion lymphoma cells were obtained from low-speed centrifugation, and pulled down with GST or GST-SIM glutathione beads. The precipitated proteins were separated on SDS-PAGE, following in-gel tryptic digestion, peptides isolated, and purified prior to MALDI-TOF-MS analysis. (B) Digital scan of SDS-PAGE separation of the LANA^{SIM}-precipitated proteins. (Top panel) Schematic representation of the LANA^{SIM} with GST fusion; Coomassie staining of SDS-PAGE of GST or GST-SIM (SIM) pulled-down proteins with two gradient elution conditions.

(Amersham Biosciences). The carboxy-terminal (945–1162) and amino terminal (1–340) mutants of LANA (referred as LANA^{NC}) tagged with GST were also performed similarly in the previous study [20]. For pull-down assay, cell NEs were individually incubated with GST or the relevant GST fusion proteins loaded on beads for 3 h at 4°C in NETN-binding buffer (50 mM Tris–HCl pH 7.5, 100 mM NaCl, 10 μm $ZnCl_2$, 10% glycerol, freshly supplemented with 0.1 mM Dithiothreitol and protease inhibitors). After washing, bound proteins were eluted with SDS sample buffer and analyzed by gel electrophoresis followed by Coomassie staining.

2.3 Gel slice preparation and MS

Twenty micrograms of total bound proteins were separated on a 4–15% precast gel (BioRad). The gel was Coomassie stained, and the lanes in the LANA^{SIM} and control samples were individually cut into six equal-sized pieces using an in-house cutting device. Protein standard bands served as a guide for the excision of gel slices of various molecular weight size ranges (40-50, 60–80, 90–100, 110–130, 140–170, and 200–300 kDa; Fig. 1). The excised gel pieces were subjected to washing with 100 μL of 50 mM ammonium bicarbonate in 50% ACN, and dehydrated in ACN followed by solvent removal using a vacuum centrifuge. Samples were then swollen in 100 μL of a digestion buffer containing 50 mM ammonium bicarbonate, 5 mM calcium chloride (50 μL), and 12.5 ng/mL of trypsin for overnight digestion. Peptides were extracted into 20 mM ammonium bicarbonate (100 μL) followed by two separate extractions into 100 μL of water/ACN/formic acid (10:10:1, v/v/v). Extracted peptides were resuspended in 10 μL of 5% ACN and 0.1% TFA, run on a MALDI-TOF) mass spectroscopy (Applied Biosystems).

2.4 Protein identification and data analysis

Peptide matches were identified by MALDI-TOF-mass spectroscopy for molecular weight determination and MALDI-TOF/TOF for sequence information and nano-LC/Qstar-XL (Applied Biosystems) analysis. The data were analyzed with GPS explorer/Analyst QS software and searched with Mascot software (Matrix Science Ltd.) against the National Center for Biotechnology Information database (NCBI). The proteins with MudPIT score with a cut-off above 40 were selected for analysis. Over twofold peptide absolute counts from LANA^{SIM} than control samples with twice repeats were selected for analysis. Based on the proteomics band analysis and the whole genome protein–protein interaction network in humans [21–23], both core network (119 genes) and extended network (49 456 genes) were constructed for all gel slices analyzed. In the core network, two interaction partners are in the corresponding proteomics slice. The interaction

relationships in the extend network had at least one interaction partner. Moreover, pathway and function annotation information were downloaded from MSigDB [24]. Then, enrichment analysis was fulfilled between the core and extended network and all the current available pathway and function categories. The most significant pathways and function categories were picked out on the basis of the enrichment *p*-value. The enrichment *p*-value is calculated on the basis of the hypergeometric distribution in this study.

2.5 In vitro SUMOylation assay

All purified recombinant proteins SUMO-1/2, Aos1/Uba2, and Ubc9 proteins were purchased, and in vitro SUMOylation assay was performed according to manufacturer's instruction (Shanghai Chairmade Inc., China). Briefly, a 100 μL volume containing 100 nM Aos1/Uba2, 1.5 μM Ubc9, 10 μM mature SUMO-1/2, 50 mM Tris, 5 mM $MgCl_2$, 2 mM ATP, pH 7.5, and 0.5 μM of purified His-KAP1 was incubated for 3 h at 37°C. Reactions products were used for GST pull-down assay or directly quenched with SDS loading buffer, and subsequently analyzed by SDS-PAGE and immunoblotting.

2.6 Immunoblotting

Protein samples were separated by SDS-PAGE and transferred onto nitrocellulose membrane (Pall Corporation, USA). After blocking with 5% nonfat dry milk in PBS (2 mM KCl, 120 mM NaCl, 1.5 mM KH_2PO_4, 8 mM Na_2HPO_4) containing 0.1% Tween 20, proteins of interest were probed with the corresponding antibodies: CBP(A-22), p300(C-20), Sin3A(AK-11), DNA-PKc(18-2), and KAP1(20C1), purchased from Santa Cruz or Abcam, and RBP-Jκ(BWH39), obtained from Elliott Kieff (Harvard Medical School, Boston, USA), followed by appropriate infrared-conjugated secondary antibodies (Alexa Fluor 800 or 680), were used with the Li-COR (Lincoln, Nebraska, USA) Odyssey scanner.

2.7 Statistical analysis

Data were analyzed by the Statistical Package for Social Science software 20.0 (IBM Corp., Armonk, NY) for statistical analysis. All statistical tests were 2-tailed, and results were considered significant when *p* value is less than 0.05.

3 Results

3.1 Quantitative proteomic analysis of LANA^{SIM}-associated proteins in vitro

To determine the proteomic profile of LANA^{SIM}-associated proteins, we performed in vitro pull-down assays with NEs from KSHV-positive BC-3 cells. NEs were incubated with glutathione-conjugated beads bound to the recombinant protein of GST fused with the SIM motif of LANA, followed by MALDI-TOF MS analysis and protein sequencing identification (Fig. 1A). With two gradient washing conditions for GST beads, six specific bands of LANA^{SIM}-associated proteins were consistently observed in Coomassie-stained gel as our previous studies (see Fig. 1B and [11]). Compared with the parallel samples from GST control, 151 proteins were exclusively identified by MS/MS analysis as significantly associated with LANA^{SIM} (over twofold, $p < 0.05$) (Table 1).

3.2 Comparison between LANA^{SIM}- and LANA^{NC}-associated proteomic profiles

To investigate whether there are some identified protein overlap between the LANA^{SIM}-associated proteome profile and the LANA^{NC}-associated proteome profile reported previously [20], we aligned each protein within the LANA^{SIM} and LANA^{NC} profiles. Surprisingly, there is only one protein namely DNA-PKc that was identified in both LANA^{SIM} and LANA^{NC} profiles, while most proteins were exclusive for each of their independent profiles (Fig. 2A).

To address in further detail the difference between the LANA^{SIM} and LANA^{NC} profiles in terms of their relationship to the SUMO pathway, we analyzed the percentage of SUMOylated and non-SUMOylated proteins in each profile through computational prediction of the number of proteins containing the consensus φKxE or noncanonical SUMOylation site. Interestingly, as shown in Fig. 2B, in the LANA^{SIM}-associated profile, 92.7% identified proteins have a high potential for being SUMOylated, while relatively lower number (86.7%) was identified in the LANA^{NC}-associated profile. In contrast, the ratio of proteins containing only the consensus φKxE (21.1%) or noncanonical (40.8%) SUMOylated sites in the LANA^{SIM}-associated profile were significantly higher (about 2-fold) than that in the LANA^{NC}-associated profile (7.8 and 23%, respectively). Unexpectedly, the majority of the SUMOylated proteins (35% and 48%) in the LANA^{SIM}-associated profile contained only one potential SUMOylation site, while most of the potential SUMOylated proteins (43% and 62%) from the LANA^{NC}-associated profile contained over three SUMOylation sites (Fig. 2C).

To determine if the SUMOylated proteins in the LANA^{SIM}-associated profile require an increase in the number of SIM motifs, we analyzed the percentage of proteins with different number of SIM motifs (0, 1, 2, 3, >3) in LANA^{SIM} and LANA^{NC} profiles by setting the conserved residues V/I-X-V/I-V/I as a SIM motif. Consistent with our hypothesis, the results showed that over 50% of the proteins in the LANA^{SIM} profile include at least one SIM motif, while only 16.9% of the proteins in the LANA^{NC} profile contained SIM motif (Fig. 2D). Moreover, the correlation analysis of the number of SIM motif and SUMOylated sites within the same protein revealed that the LANA^{SIM} and LANA^{NC} associate with

Table 1. The characters of LANA^{SIM}-associated proteins identified by MS

Gene symbol	SUMOylated site	Gene description	kDa/p*I*	Queries matched	Significance threshold $p < 0.05$	Core pathway (P) or function (F) listed in Fig. 3B and C
SMC1A	Y	Structural maintenance of chromosomes 1A	143/7.51	18	5.625	P9, P4, P2, P7
MCM4	Y	Minichromosome maintenance complex component 4	97/6.28	5	2.525252525	P9, P8, P6, P7, P5
MCM3	Y	Minichromosome maintenance complex component 3	91/5.53	8	7.476635514	P9, P8, P6, P7
MCM7	Y	Minichromosome maintenance complex component 7	81/6.08	10	3.448275862	P9, P8, P6, P7
MCM5	Y	Minichromosome maintenance complex component 5	82/8.71	39	3.797468354	P9, P8, P6, P7
MCM6	Y	Minichromosome maintenance complex component 6	93/5.31	11	26.82926829	P9, P8, P6, P7
SMC3	Y	Structural maintenance of chromosomes 3	142/6.77	2	2.53164557	P9, P7
CUL1	Y	Cullin 1	90/8.19	23	5.437352246	P9, P7
SMC1B	Y	Structural maintenance of chromosomes 1B	144/7.69	1	1.612903226	P9,
P300	Y	E1A-binding protein p300	264/8.81	28	8.777429467	P9, P3, P1, P5, F2, F4
CBP	Y	CREB-binding protein	265/8.83	67	5.0413845	P9, P3, P1, P5, F2, F4
DNAPKC	Y	Protein kinase, DNA-activated, catalytic polypeptide	469/6.75	463	6.103348273	P9,
NUP133	Y	Nucleoporin 133 kDa	129/4.98	2	4.444444444	P9, P4, P7
NUP155	Y	Nucleoporin 155 kDa	155/5.78	25	4.504504505	P4, P2
NUP93	Y	Nucleoporin 93 kDa	93/5.5	14	4.794520548	P4, P2
NCBP1	Y	Nuclear cap binding protein subunit 1, 80 kDa	92/5.99	4	4.938271605	P4, P2
SF3B1	Y	Splicing factor 3b, subunit 1, 155 kDa	146/6.65	10	6.134969325	P4, P2
HNRNPU	Y	Heterogeneous nuclear ribonucleoprotein U (scaffold attachment factor A)	91/5.76	5	7.042253521	P4, P2
DHX9	Y	DEAH (Asp-Glu-Ala-His) box polypeptide 9/RNA helicase A	141/6.41	1	2.222222222	P4, P2, F1, F3, F5, F6, F7, F9, F10
HNRNPH1	Y	Heterogeneous nuclear ribonucleoprotein H1	49/5.89	11	2.095238095	P4, P2
ADAR	Y	Adenosine deaminase, RNA specific	136/8.86	20	3.731343284	P4,
HSP90AA1	Y	Heat shock protein 90 kDa alpha (cytosolic), class A member 1	85/4.94	14	4.057971014	P9, P7, P1
TUBG1	Y	Tubulin, gamma 1	51/5.75	7	7.865168539	P9, P7, F8
RUVBL2	Y	RuvB-like 2	51/5.49	10	5	P9, P1, F1, F3, F6, F7, F9
SIN3A	Y	SIN3 homolog A, transcription regulator	145/6.82	115	5.512943432	P3, P5
SIN3B	Y	SIN3 homolog B, transcription regulator	133/6.48	6	10.16949153	P3
CPT1A	Y	Carnitine palmitoyltransferase 1A (liver)	88/8.85	3	2.272727273	P3, F2, F4
MED16	Y	Mediator complex subunit 16	97/7.12	2	1.492537313	P3
HADHA	Y	Hydroxyacyl-CoA dehydrogenase/3-ketoacyl-CoA thiolase/ enoyl-CoA hydratase (trifunctional protein), alpha subunit	83/9.16	4	2.051282051	P3, F2, F4

Table 1. Continued

Gene symbol	SUMOylated site	Gene description	kDa/p*I*	Queries matched	Significance threshold $p < 0.05$	Core pathway (P) or function (F) listed in Fig. 3B and C
HADHB	Y	Hydroxyacyl-CoA dehydrogenase/3-ketoacyl-CoA thiolase/enoyl-CoA hydratase (trifunctional protein), beta subunit	51/9.45	18	4.774535809	P3, F2, F4
ACLY	Y	ATP citrate lyase	121/6.95	2	2.083333333	P3, F2
EIF4A1	N	Eukaryotic translation initiation factor 4A1	46/5.32	59	2.912142152	P1
RCC1	N	Regulator of chromosome condensation 1	13/7.90	25	3.41997264	P1
KAT2A	Y	K(lysine) acetyltransferase 2A	94/9.18	7	5.64516129	P1
COPA	Y	Coatomer protein complex, subunit alpha	138/7.70	41	5.466666667	P5
KAP1	Y	Tripartite motif containing 28(TRIM28)/TIF1B	89/5.52	19	3.025477707	P5
SND1	Y	Staphylococcal nuclease and tudor domain containing 1	102/6.74	7	14.89361702	P5
PIK3R4	Y	Phosphoinositide-3-kinase, regulatory subunit 4	153/6.74	2	4.255319149	
HSD17B4	Y	Hydroxysteroid (17-beta) dehydrogenase 4	80/8.96	13	3.430079156	
SMPD4	Y	Sphingomyelin phosphodiesterase 4, neutral membrane (neutral sphingomyelinase-3)	93/8.11	2	2.409638554	
COPB1	Y	Coatomer protein complex, subunit beta 1	107/5.72	12	6.18556701	
COPG	Y	Coatomer protein complex, subunit gamma	98/5.32	10	2.136752137	
COPB2	Y	Coatomer protein complex, subunit beta 2 (beta prime)	102/5.14	3	6.666666667	
SEC31A	Y	SEC31 homolog A	133/6.43	1	1.754385965	
SEC23A	Y	Sec23 homolog A	86/6.64	2	2.083333333	
SEC24C	Y	SEC24 family, member C	118/6.71	1	1.851851852	
DDOST	Y	Dolichyl-diphosphooligosaccharide–protein glycosyltransferase	51/6.09	6	9.677419355	
ATP5A1	Y	ATP synthase, H+ transporting, mitochondrial F1 complex, alpha subunit 1, cardiac muscle	60/9.16	53	4.305442729	
ATP5B	N	ATP synthase, H+ transporting, mitochondrial F1 complex, beta polypeptide	57/5.26	16	3.368421053	
EIF3B	Y	Eukaryotic translation initiation factor 3, subunit B	92/4.89	4	4.347826087	
EIF3C	Y	Eukaryotic translation initiation factor 3, subunit C	105/5.48	18	4.864864865	
EIF3F	N	Eukaryotic translation initiation factor 3, subunit F	38/5.24	4	1.234567901	
EEF2	Y	Eukaryotic translation elongation factor 2	95/6.41	17	4.381443299	
EEF1A1	Y	Eukaryotic translation elongation factor 1 alpha 1	50/9.10	61	6.517094017	
HK1	Y	Hexokinase 1	102/6.44	34	7.112970711	
ABCB1	Y	ATP-binding cassette, subfamily B (MDR/TAP), member 1	141/9.06	2	2.43902439	
EGLN1	N	egl nine homolog 1	46/8.83	4	1.895734597	

Table 1. Continued

Gene symbol	SUMOylated site	Gene description	kDa/p*I*	Queries matched	Significance threshold $p < 0.05$	Core pathway (P) or function (F) listed in Fig. 3B and C
PFKL	Y	Phosphofructokinase, liver	85/7.26	4	6.349206349	
EIF4A3	Y	Eukaryotic translation initiation factor 4A3	47/6.30	28	6.222222222	F1, F3, F5, F6, F7, F9, F10
ECSIT	N	ECSIT homolog	49/5.89	3	3.529411765	
SUPT16H	Y	Suppressor of Ty 16 homolog	120/5.50	2	3.174603175	
XRCC5	Y	ATP-dependent DNA helicase II / X-ray repair complementing defective repair in Chinese hamster cells 5 (double-strand break rejoining)	83/5.55	57	9.223300971	F1, F3, F6, F7, F9
RRM1	Y	Ribonucleotide reductase M1	90/6.76	4	5.797101449	
UQCRC1	N	Ubiquinol–cytochrome c dehydrogenase core protein I	53/5.94	8	10.66666667	
UQCRC2	Y	Ubiquinol–cytochrome c reductase core protein II	48/8.74	37	2.324120603	
NNT	Y	Nicotinamide nucleotide transhydrogenase	114/8.31	1	2.127659574	
PDK3	Y	Pyruvate dehydrogenase kinase, isozyme 3	47/8.46	2	1.98019802	
DIS3	Y	DIS3 mitotic control homolog	109/6.69	1	2.325581395	
DDX6	Y	DEAD (Asp-Glu-Ala-Asp) box polypeptide 6/RCK	54/8.85	9	6.474820144	F1, F5
ATP2A2	Y	ATPase, Ca++ transporting, cardiac muscle, slow twitch 2	110/5.25	2	1.869158879	F3, F6, F9
HSPA1L	Y	Heat shock 70 kDa protein 1-like	70/5.75	10	1.592356688	
KRT1	Y	Keratin 1	66/8.16	9	13.04347826	F8
ILKAP	Y	Integrin-linked kinase-associated serine/threonine phosphatase	43/6.68	2	2.702702703	
PDIA6	Y	Protein disulfide isomerase family A,member 6	48/4.95	2	3.076923077	
PLG	N	Plasminogen	91/6.89	10	18.51851852	
TTC37	Y	Tetratricopeptide repeat domain 37	175/7.47	2	2.702702703	
PA2G4	Y	Proliferation-associated 2G4, 38 kDa	44/6.13	19	4.148471616	
NCAPD2	Y	Non-SMC condensin I complex, subunit D2	157/6.19	6	2.189781022	
SMC2	Y	Structural maintenance of chromosomes 2	41/9.22	10	3.012048193	
NOC2L	Y	Nucleolar complex associated 2 homolog	85/5.46	1	1.851851852	
DDX17	Y	DEAD (Asp-Glu-Ala-Asp) box polypeptide 17, Isoform 1	80/8.53	2	4.87804878	F1, F3, F5, F6, F9, F10
SERPINH1	Y	Serpin peptidase inhibitor, clade H (heat shock protein 47), member 1, (collagen binding protein 1)	46/8.75	1	1.639344262	
OBSCN	Y	Obscurin, cytoskeletal calmodulin and titin-interacting RhoGEF	868/5.69	4	8.888888889	
PICK1	Y	Protein interacting with PRKCA 1	47/5.17	1	2.222222222	F3, F9
CYFIP1	Y	Cytoplasmic FMR1 interacting protein 1	145/6.46	19	4.822335025	

Table 1. Continued

Gene symbol	SUMOylated site	Gene description	kDa/p*I*	Queries matched	Significance threshold $p < 0.05$	Core pathway (P) or function (F) listed in Fig. 3B and C
ALDH18A1	Y	Aldehyde dehydrogenase 18 family, member A1	87/6.66	70	3.575076609	
TUFM	Y	Tu translation elongation factor, mitochondrial	50/7.26	8	2.816901408	
MTHFD1	N	Methylenetetrahydrofolate dehydrogenase (NADP+ dependent) 1, methenyltetrahydrofolate cyclohydrolase, formyltetrahydrofolate synthetase	102/6.89	79	4.867529267	
VARS	N	Valyl-tRNA synthetase	140/7.53	8	2.067183463	
KRT19	Y	Keratin 19	44/5.05	3	3.333333333	F8
DDX39A	Y	Nuclear RNA helicase / DEAD (Asp-Glu-Ala-Asp) box polypeptide 39A	49/5.46	36	3.614457831	F1, F3, F5, F6, F7, F9, F10
GCN1L1	Y	GCN1 general control of amino-acid synthesis 1-like 1	293/7.29	3	4.109589041	
IMMT	Y	Inner membrane protein, mitochondrial	84/6.08	18	4.295942721	
LOH12CR1	Y	Loss of heterozygosity, 12, chromosomal region 1	17/5.48	28	36.84210526	
PDS5A	Y	PDS5, regulator of cohesion maintenance, homolog A	151/8.15	8	12.12121212	
NOMO1	Y	NODAL modulator 1	134/5.54	3	3.947368421	
TARDBP	Y	TAR DNA-binding protein	45/5.85	2	1.142857143	
LEMD3	Y	LEM domain containing 3	110/7.32	12	1.829268293	
INTS7	Y	Integrator complex subunit 7	107/8.30	1	1.428571429	
ABHD12	Y	Abhydrolase domain containing 12	45/8.87	2	3.03030303	
CHAMP1	Y	Chromosome alignment maintaining phosphoprotein 1	89/8.70	1	2.222222222	
SLC25A24	Y	Solute carrier family 25 (mitochondrial carrier; phosphate carrier), member 24	53/6.00	6	1.511335013	
KRT2	Y	Keratin 2	65/8.07	8	5.161290323	F8
KRT6B	Y	Keratin 6B	60/8.09	1	2.173913043	F8
KRT9	Y	Keratin 9	62/5.14	14	4.166666667	F8
KRT10	Y	Keratin 10	60/5.17	13	5.752212389	
DCAF8	Y	DDB1- and CUL4-associated factor 8	66/5.05	11	16.17647059	
SCCPDH	N	Saccharopine dehydrogenase (putative)	47/9.24	2	3.636363636	
CCDC87	Y	Coiled-coil domain containing 87	96/8.74	4	6.349206349	
VPS35	Y	Vacuolar protein sorting 35 homolog	92/5.32	4	4.494382022	
UNC45A	Y	unc-45 homolog A	103/5.80	1	1.388888889	
ZC3HAV1	Y	Zinc finger CCCH-type, antiviral 1	101/8.72	1	2.040816327	
ATP13A1	Y	ATPase type 13A1	133/8.46	1	2.222222222	
SCYL1	Y	SCY1-like 1	90/5.93	2	4.545454545	

Table 1. Continued

Gene symbol	SUMOylated site	Gene description	kDa/p*I*	Queries matched	Significance threshold $p < 0.05$	Core pathway (P) or function (F) listed in Fig. 3B and C
RGL2	Y	ral guanine nucleotide dissociation stimulator-like 2	85/5.82	4	8	
INTS3	Y	Integrator complex subunit 3	118/5.53	8	16.66666667	
SUPV3L1	Y	Suppressor of var1, 3-like 1	88/8.2	14	2.417962003	F1
SPAG16	Y	Sperm associated antigen 16	71/5.90	4	8.163265306	
NAA15	Y	*N*(alpha)-acetyltransferase 15, NatA auxiliary subunit	101/7.23	6	10	F2, F4
SLC13A3	Y	Solute carrier family 13 member 3	69/8.87	5	10.41666667	
TMEFF1	Y	Transmembrane protein with EGF-like and one follistatin-like domain	41/6.59	19	45.23809524	
FLJ00119	Y	FLJ00119 protein	154/5.49	3	3.225806452	
UBC	N	Polyubiquitin-C	68/7.13	4	5.263157895	
SMC2	Y	Structural maintenance of chromosomes 2	41/9.22	10	3.012048193	
MYO6	Y	Unconventional myosin-VI	150/8.74	13	4.850746269	
MSH6	Y	DNA mismatch repair protein Msh6	153/6.50	9	8.737864078	
ABCB1	Y	Multidrug resistance protein 1	141/9.06	2	2.43902439	
SAP130	Y	Sin3A-associated protein, 130kDa, isoform CRA_c	73/10.52	1	1.754385965	
EIF4G2	Y	Eukaryotic translation initiation factor 4 gamma 2	102/6.69	15	6.912442396	
OCRL	Y	Inositol polyphosphate 5-phosphatase OCRL-1	104/6.13	1	1.724137931	
KRT1	Y	Keratin, type II cytoskeletal 1	66/8.15	6	12.5	
SCYL1	Y	N-terminal kinase-like protein	90/5.93	2	4.545454545	
NSF	Y	NSF protein	36/5.50	10	3.623188406	
DKFZp586L0518	Y	Putative uncharacterized protein DKFZp586L0518	16/6.56	3	5.172413793	
POLDIP3	N	POLDIP3 protein	25/10.69	8	3.375527426	
FAM175A	Y	FAM175A protein	8/8.48	2	4.347826087	
SUV3	Y	Putative ATP-dependent mitochondrial RNA helicase	88/8.2	14	2.41796	

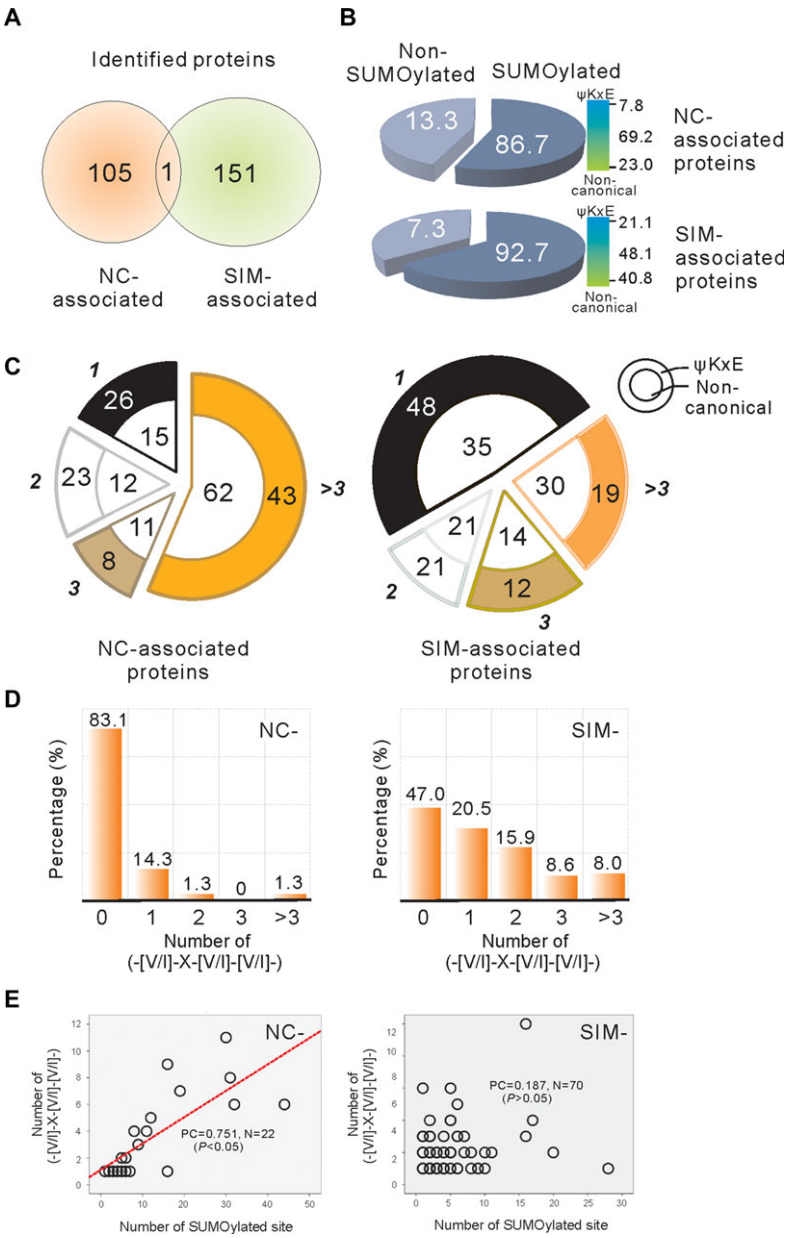

Figure 2. The differential proteome profiles of LANA^{SIM}- and LANA^{NC}-associated proteins. (A) Venn diagram of identified proteins from LANA^{SIM}- or LANA^{NC}-associated proteins by MS. The number is obtained based on peptides of the proteins detected from mass spectrum. (B) The relative percentage of SUMOylated and non-SUMOylated proteins associated with LANA^{SIM} or LANA^{NC}. The relative percentage was calculated according to the number of protein containing ΨKxE or noncanonical consensus SUMOylated sites, which predicated by SUMOsp_2.0.4_ windows_20090805.exe (software download from http:// sumosp.biocuckoo.org/download.php), threshold setting is medium. The ratio of protein containing only ΨKxE, noncanonical consensus, or both among the SUMOylated proteins is individually shown in the histogram on the right panels. (C) The relative percentage of LANA^{SIM}- or LANA^{NC}-associated proteins with different number (1, 2, 3, >3) of ΨKxE (outer circle) or noncanonical consensus (inner circle) SUMOylated sites, and (D) of the -[V/I]-X-[V/I]-[V/I]- consensus SIM motifs. (E) The number correlation of SIM motif and SUMOylated site within the same proteins from the SIM- or NC-associated proteins was analyzed by Statistical Package for Social Science software. The dot line denotes the potential correlation between the number of SIM motif and SUMOylated site within the same proteins. PC, Pearson correlation.

two different populations of SUMOylated proteins (Fig. 2E). Taken together, this indicates that LANA^{SIM} domain can recruit more specific SUMO-associated proteins compared to LANA^{NC}.

3.3 The core network of LANA^{SIM}-associated proteins

To better understand which cellular signal pathways and related functions were modulated by proteins associated with LANA^{SIM}, we clustered the LANA^{SIM}-associated proteome by alignment with over 45 000 genes related to cellular signal pathways. The results revealed that 119 proteins of the LANA^{SIM}-related profiles that were matched in the network were linked to translational initiation factor EIF4A, heat shock protein 90, and the SCF ubiquitin-complex scaffold protein Cullin1 (Cul1) as the core proteins (Fig. 3A). In the specific core signaling pathways, the LANA^{SIM}-associated proteins are mainly involved in the regulation of cell cycle (particularly mitotic), DNA unwinding and replication, and pre-mRNA/mRNA processing, while some are involved in c-myc/c-myb transcription activation network and several metabolic pathways such as fatty acids, triacylglycerols, and ketones (Fig. 3B). Consistently, the results of functional analysis showed that the majority of LANA^{SIM}-associated proteins belong to the identified core pathway-related enzymes, which include helicases, ATPases,

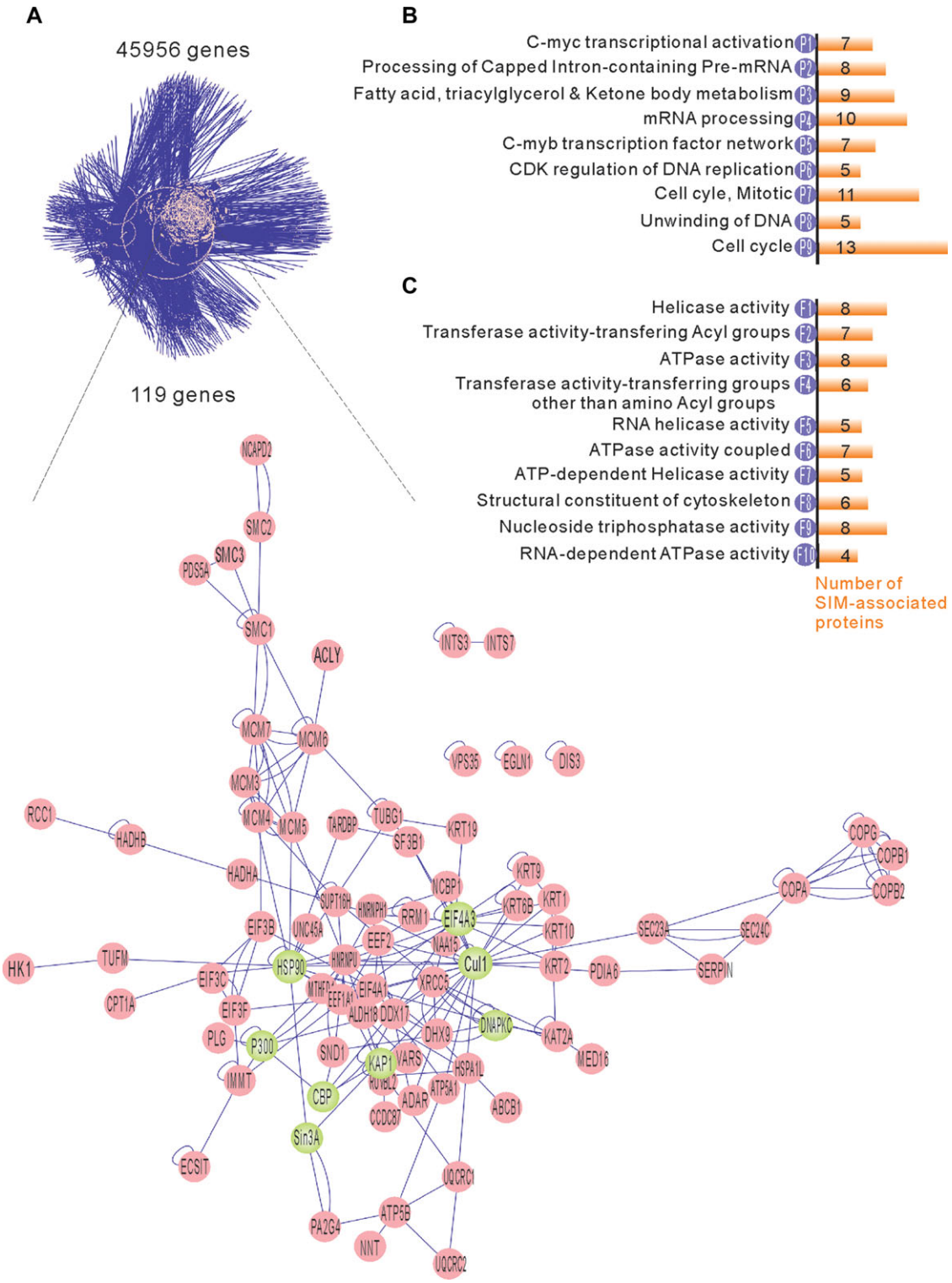

Figure 3. Ingenuity analysis of representative proteins from the LANA^{SIM}-associated complex. (A) Hypothetical LANA^{SIM} regulatory circuit. LANA^{SIM} initiates the 119 genes circuit via Cul1 (SCF ubiquitin complex scaffold) and heat shock protein 90. Total 45956 genes in extended network were collected, analyzed, and compared for overlaps with LANA^{SIM}-associated proteins. Zoom-in of the core network with LANA^{SIM} interconnected hubs is displayed. Green nodes denote proteins significantly enriched by LANA^{SIM} and with more counts of peptide hits detected by MS. (B) The cellular pathways and (C) functional clustering analysis of the identified proteins from LANA^{SIM}-associated complex.

acyl group transferases, and nucleoside triphosphatases (Fig. 3C).

3.4 SUMO2-modified molecules are essential components of the LANA^{SIM}- associated proteome

To further validate the potential associations of the identified LANA^{SIM}-associated proteins in complex with LANA^{SIM}, we selected five major genes including CBP, p300, DNA-PKc, Sin3A, and KAP1 (four was previously reported to be SUMOylated [25–28]), and performed in vitro pull-down assays by the incubation of HEK293 cell NE with GST-fused LANA^{SIM} or GST proteins. The RBP-Jκ (a well-known LANA-interacting protein [29]) and LANA$_{1\text{-}329}$ΔSIM (the deleted mutant of SIM motif at amino terminus of LANA) were used as controls. The results showed that these proteins including CBP, p300, DNA-PKc, Sin3A, KAP1, and RBP-Jκ did associate with LANA through the SIM motif at some extent (Fig. 4A). Interestingly, the modified isoforms of both CBP and RBP-Jκ proteins with high molecular weight was also greatly presented in the LANA^{SIM}-associated complex. This strongly suggests that the identified profile of the LANA^{SIM}-associated proteome is specific.

To address if SUMOylated molecules are critical partner in the LANA^{SIM}-associated complex when looking at the total LANA^{SIM}-associated protein profile, we found that chromatin remodeler KAP1 (which was shown to be a SUMO E3 ligase [30]) is one of the identified proteins (above 5% peptide matched) from our MS analysis (Fig. 4B). Although our previous studies have shown that the SUMO-2-modified isoform of KAP1 is a key partner of LANA^{SIM} in vivo [11], it remains unknown if the SUMO-2-modified KAP1 does directly bind to the SIM motif of LANA independent of other molecules. To address this question, we performed pull-down assays using in vitro SUMOylated KAP1 with GST-fused wild-type LANA1-329 or its SIM-deleted mutant, respectively. As shown in Fig. 4C, we observed that the SUMO2-modified KAP1 (KAP1-SUMO2) did have a much higher affinity with LANA^{SIM} than the SUMO1-modified KAP1 (KAP1-SUMO1). However, the amino terminus of LANA in the absence of SIM motif was able to interact with native KAP1. This indicates that SUMO-2-modified KAP1 is preferential to bind with the SIM motif of LANA.

4 Discussion

The MALDI-TOF mass spectrum is a powerful technology for studying the distribution and in situ identification of the molecular machinery within biological tissues with no specific requirement of predefined targets [31]. It is therefore possible to identify the proteomic profile of protein–protein interactions of a protein of interest. To globally address the biological role of LANA in KSHV-mediated latent infection and pathogenesis, several proteomic assays to identify LANA-interacting proteins have been carried out recently by different procedures to address specific questions [20, 32–34]. However, it is difficult to identify the same LANA-interacting proteins using different proteomic assays, which could be due to the possibilities of using different cell type, expression system, or truncated mutants of LANA. To elucidate the proteomic specificity of the LANA^{SIM} profile, we determined the difference between the LANA^{SIM}- and the LANA^{NC}- associated proteome identified by MS. Unexpectedly, we found that only the DNA-activated protein kinase DNA-PKc appeared in the profiles of both LANA^{SIM}- and LANA^{NC}-associated proteome. This suggests that the LANA^{SIM}-associated proteins have great specificity. The reason why the low overlap of identified proteins between the LANA^{SIM}- and LANA^{NC} -associated proteome could be due to the different enrichment levels of LANA^{SIM} and LANA^{NC} targeting proteins, as well as other unclassified proteins. Nonetheless, there is few protein overlap between the LANA^{SIM}- and LANA^{NC}- associated proteome profiles. Analysis of the functional category of identified proteins revealed that the LANA^{SIM} and LANA^{NC} polypeptides recruit similar functional activities of proteins including ATPases (LANA^{NC}: DD16; LANA^{SIM}: ATP2A2, ATP13A1, ATP synthase ATP5A1 and ATP5B), RNA helicases (LANA^{NC}: DD16; LANA^{SIM}: DHX9, XRCC5, SUV3, DDX17, DDX39A, and DDX6), chaperon (LANA^{NC}: DJC8, nucleophosmin; LANA^{SIM}: heat shock protein 90, Hsp70L), and cytoskeleton (LANA^{NC}: merlin, moesin, periplakin, nebulin; LANA^{SIM}: keratin1, keratin 2, keratin 6B, keratin 9, keratin 10, keratin 19) [20]. In addition, although the proteins from the LANA^{NC} or LANA^{SIM} complexs are different, they are involved in the similar cellular processes, particularly cell cycle control, pre-mRNA splicing regulation, and ubiquitin proteasome pathway. For instance, LANA^{NC} profile contains ubiquitin proteasome system protein FX16 [20], while the LANA^{SIM} profile includes Cul1, DDB1, and CUL4-associated factor 8. These strengthen our hypothesis that the LANA^{SIM} motif is a functional domain of LANA in modulating cellular processes.

Notably, cytokine and ribosomal subunits were included in the LANA^{NC} -associated protein profile but not in the LANA^{SIM} -associated protein profile, while the LANA^{SIM} exclusively interacted with eukaryotic translation initiation factors (EIF3B, EIF3C, EIF3F, EIF4A3, EIF4G2), translation elongation factor (EEF2, EEF1A1), minichromosome maintenance complex (MCM3, MCM4, MCM5, MCM6, MCM7), structural maintenance complex of chromosomes (SMC1A, SMC3, SMC2, SMC1B), and nucleoporin (NUP133, NUP155, NUP93), indicating that the LANA^{SIM} motif is important for regulating cellular process involved with protein translation initiation and elongation, chromosome maintenance, as well as nucleus–cytoplasm trafficking.

It should be mentioned that consistent with our discovery of LANA^{SIM} and its importance for interaction with SUMO molecules, the recent reports by other groups have shown that both SUMO-1 and SUMO-3 also appears in the

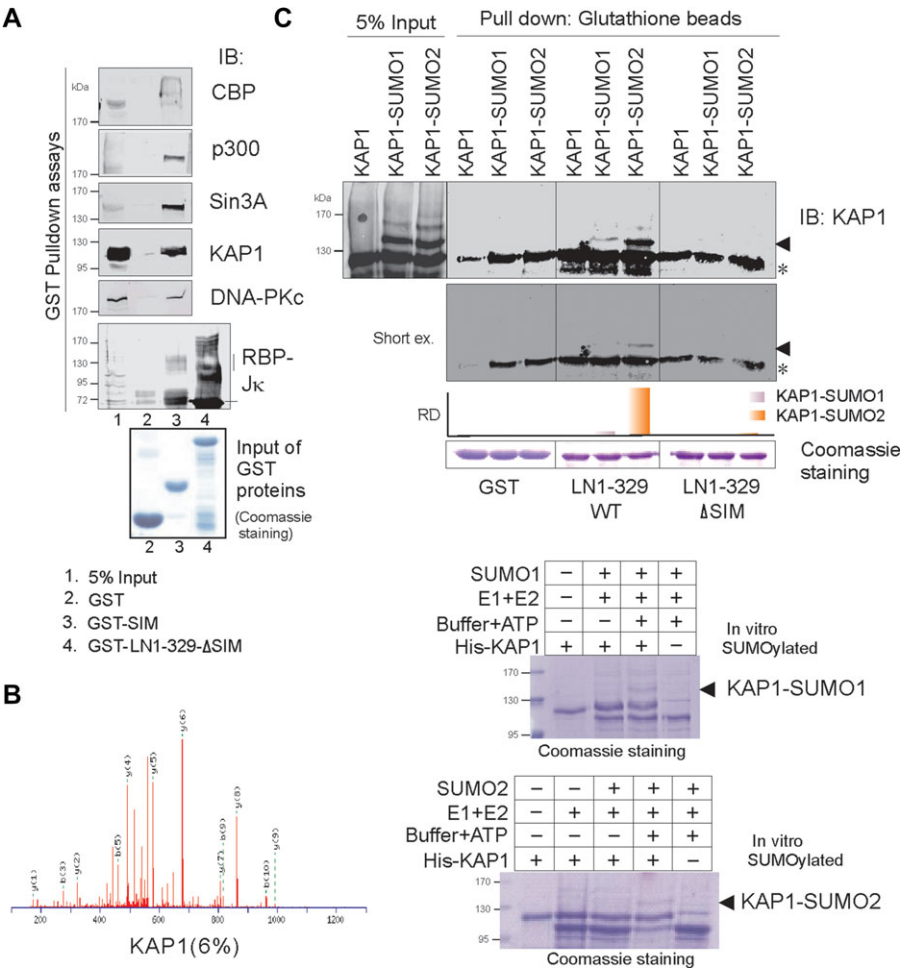

Figure 4. Validation of representative cellular SUMOylated proteins associated with LANA^{SIM}. (A) Binding assays of the LANA^{SIM}-associated proteomic identified proteins in vitro. Purified GST, GST-SIM, or GST-LN1-329ΔSIM was incubated with HEK293 cell nuclear extract. Captured on Glutathione (GSH)–sepharose beads and analyzed by immunblotting (IB) with indicated antibodies. An aliquot of cell nuclear extract was also applied directly to the gel (Input). The GST fusion proteins were visualized on the blot by Coomassie staining (bottom panel). (B) Representative and overlap percentage of identified KAP1 peptides from MS/MS spectrum. (C) LANA^{SIM} presents higher directly affinity with SUMO2-modified than SUMO1-modified KAP-1 in vitro. Equal protein amount of in vitro SUMOylated KAP1 with SUMO-1 (KAP1-SUMO-1) or SUMO-2 (KAP1-SUMO-2) was individually obtained according to Materials and Methods section (top panels), and subjected to pull-down assays with GST, GST-LN1-329, or GST-LN1-329ΔSIM as previously described. The relative density (RD) of KAP1-SUMO-1 and KAP1-SUMO-2 binding per input is shown. The asterisk denotes the nonspecific binding of GST with native KAP1. The GST fusion proteins were visualized on the blot by Coomassie staining (bottom panel).

LANA complex by using protein array screening and tandem affinity purification-MS, respectively [32, 33]. Moreover, supporting our hypothesis, the ratio of SUMOylated proteins with SIM motif simultaneously in the LANA^{SIM} profile was much higher than that seen in the LANA^{NC} profile (92.7% × 53% = 49.1% vs. 86.7% × 16.9% = 14.6%). This could be due to the fact that the SIM motif can specifically enrich the SUMOylated proteins. For instance, although the LANA^{SIM}-associated proteins contain less SUMOylated site than the LANA^{NC}-associated proteins (48 vs. 26% for only one), among the LANA^{SIM-}associated proteins, 92.7% could be SUMOylated and over half of them containing one or more SIMs, while only 86.7% and about 16% among the LANA^{NC}-associated proteins, respectively. This indicates that both SUMOylated and a SIM motif are key for a protein to associate with LANA^{SIM}. The results of LANA^{SIM}-associated proteome profile include CBP/P300, Sin3A, RBP-Jκ, and KAP1, which have been previously identified as SUMOylated proteins [29, 33, 35, 36], further support our conclusion that the LANA^{SIM} motif is specifically associated with SUMOylated proteins. Furthermore, our data not only proved that SUMO-2 directly associated with the LANA^{SIM} motif in vitro, but also showed that SUMO-1 or SUMO-2 modification of KAP1 reduced its affinity to nonspecifically bind to GST compared with native KAP1. Although the reaction system of in vitro SUMOylation enhances the nonspecific affinity of GST interaction with KAP1, this could be due to E1 or E2 enzymes acting as a linker and has not been fully explored at this time.

In summary, our proteomic analysis identified a number of known LANA^{SIM} interacting proteins and has significantly expanded the number and functional categories of proteins associated with LANA. A large number of potentially SUMOylated proteins were identified that have important roles in KSHV latency, specifically the regulation of cell cycle, DNA replication, mRNA processing, and chromosome maintenance. The LANA^{SIM} motif therefore forms complexes with SUMOylated and non-SUMOylated proteins belonging to several defined functional classes. This expanded view of cellular interacting proteins may present additional functions involved in KSHV pathogenesis. However, further investigations utilizing exogenous expression systems or siRNA-mediated specific individual gene knockdown are required to identify the coupling of functions linked to some of the LANA^{SIM}-associated proteins important for KSHV latency.

This may also serve as potential drug targets against KSHV-associated diseases.

This work was supported by the Key Program of the Shanghai Municipal Education (13zz011), the National Natural Science Foundation of China (81471930, 81402542), and the National Key Basic Research Program of China (2012CB519001). F.W. is a scholar of Pujiang Talents in Shanghai. Q.C. is a scholar of New Century Excellent Talents in University of China. Public health grants from the NIH (R01CA919972, R01DE017338, R01CA171979, and P01CA174439) to E.S.R. also supported this work.

The authors have declared no conflict of interest.

5 References

[1] Flotho, A., Melchior, F., Sumoylation: a regulatory protein modification in health and disease. *Annu. Rev. Biochem.* 2013, *82*, 357–385.

[2] Sarge, K. D., Park-Sarge, O. K., Sumoylation and human disease pathogenesis. *Trends Biochem. Sci.* 2009, *34*, 200–205.

[3] Everett, R. D., Boutell, C., Hale, B. G., Interplay between viruses and host sumoylation pathways. *Nat. Rev. Microbiol.* 2013, *11*, 400–411.

[4] Mattoscio, D., Segre, C. V., Chiocca, S., Viral manipulation of cellular protein conjugation pathways: the SUMO lesson. *World J. Virol.* 2013, *2*, 79–90.

[5] Bohren, K. M., Nadkarni, V., Song, J. H., Gabbay, K. H., Owerbach, D., A M55V polymorphism in a novel SUMO gene (SUMO-4) differentially activates heat shock transcription factors and is associated with susceptibility to type I diabetes mellitus. *J. Biol. Chem.* 2004, *279*, 27233–27238.

[6] Seeler, J. S., Dejean, A., Nuclear and unclear functions of SUMO. *Nat. Rev. Mol. Cell Biol.* 2003, *4*, 690–699.

[7] Rodriguez, J. A., Interplay between nuclear transport and ubiquitin/SUMO modifications in the regulation of cancer-related proteins. *Semin. Cancer Biol.* 2014, *27C*, 11–19.

[8] Ren, J., Gao, X., Jin, C., Zhu, M. et al., Systematic study of protein sumoylation: development of a site-specific predictor of SUMOsp 2.0. *Proteomics 2009*, *9*, 3409–3412.

[9] Zhao, Q., Xie, Y., Zheng, Y., Jiang, S. et al., GPS-SUMO: a tool for the prediction of sumoylation sites and SUMO-interaction motifs. *Nucleic Acids Res. 2014*, *42*, W325–W330.

[10] Kerscher, O., SUMO junction-what's your function? New insights through SUMO-interacting motifs. *EMBO Rep.* 2007, *8*, 550–555.

[11] Cai, Q., Cai, S., Zhu, C., Verma, S. C. et al., A unique SUMO-2-interacting motif within LANA is essential for KSHV latency. *PLoS Pathog.* 2013, *9*, e1003750.

[12] Gareau, J. R., Lima, C. D., The SUMO pathway: emerging mechanisms that shape specificity, conjugation and recognition. *Nat. Rev. Mol. Cell Biol.* 2010, *11*, 861–871.

[13] Soulier, J., Grollet, L., Oksenhendler, E., Cacoub, P. et al., Kaposi's sarcoma-associated herpesvirus-like DNA sequences in multicentric Castleman's disease. *Blood* 1995, *86*, 1276–1280.

[14] Chang, Y., Cesarman, E., Pessin, M. S., Lee, F. et al., Identification of herpesvirus-like DNA sequences in AIDS-associated Kaposi's sarcoma. *Science* 1994, *266*, 1865–1869.

[15] Cai, Q., Verma, S. C., Lu, J., Robertson, E. S., Molecular biology of Kaposi's sarcoma-associated herpesvirus and related oncogenesis. *Adv. Virus Res.* 2010, *78*, 87–142.

[16] Mesri, E. A., Cesarman, E., Boshoff, C., Kaposi's sarcoma and its associated herpesvirus. *Nat. Rev. Cancer* 2010, *10*, 707–719.

[17] Verma, S. C., Lan, K., Robertson, E., Structure and function of latency-associated nuclear antigen. *Curr. Top. Microbiol. Immunol.* 2007, *312*, 101–136.

[18] Ballestas, M. E., Kaye, K. M., The latency-associated nuclear antigen, a multifunctional protein central to Kaposi's sarcoma-associated herpesvirus latency. *Future Microbiol.* 2011, *6*, 1399–1413.

[19] Campbell, M., Izumiya, Y., Post-translational modifications of Kaposi's sarcoma-associated herpesvirus regulatory proteins—SUMO and KSHV. *Front. Microbiol.* 2012, *3*, 31.

[20] Kaul, R., Verma, S. C., Robertson, E. S., Protein complexes associated with the Kaposi's sarcoma-associated herpesvirus-encoded LANA. *Virology* 2007, *364*, 317–329.

[21] Wu, G., Feng, X., Stein, L., A human functional protein interaction network and its application to cancer data analysis. *Genome Biol.* 2010, *11*, R53.

[22] Stelzl, U., Worm, U., Lalowski, M., Haenig, C. et al., A human protein-protein interaction network: a resource for annotating the proteome. *Cell* 2005, *122*, 957–968.

[23] Pagel, P., Kovac, S., Oesterheld, M., Brauner, B. et al., The MIPS mammalian protein-protein interaction database. *Bioinformatics* 2005, *21*, 832–834.

[24] Subramanian, A., Tamayo, P., Mootha, V. K., Mukherjee, S. et al., Gene set enrichment analysis: a knowledge-based approach for interpreting genome-wide expression profiles. *Proc. Natl. Acad. Sci. USA* 2005, *102*, 15545–15550.

[25] Girdwood, D., Bumpass, D., Vaughan, O. A., Thain, A. et al., P300 transcriptional repression is mediated by SUMO modification. *Mol. Cell* 2003, *11*, 1043–1054.

[26] Kuo, H. Y., Chang, C. C., Jeng, J. C., Hu, H. M. et al., SUMO modification negatively modulates the transcriptional activity of CREB-binding protein via the recruitment of Daxx. *Proc. Natl. Acad. Sci. USA* 2005, *102*, 16973–16978.

[27] Pungaliya, P., Kulkarni, D., Park, H. J., Marshall, H. et al., TOPORS functions as a SUMO-1 E3 ligase for chromatin-modifying proteins. *J. Proteome Res.* 2007, *6*, 3918–3923.

[28] Li, X., Lin, H. H., Chen, H., Xu, X. et al., SUMOylation of the transcriptional co-repressor KAP1 is regulated by the serine and threonine phosphatase PP1. *Sci. Signal.* 2010, *3*, ra32.

[29] Lan, K., Kuppers, D. A., Verma, S. C., Sharma, N. et al., Induction of Kaposi's sarcoma-associated herpesvirus latency-associated nuclear antigen by the lytic transactivator RTA: a novel mechanism for establishment of latency. *J. Virol.* 2005, *79*, 7453–7465.

[30] Yang, Y., Fiskus, W., Yong, B., Atadja, P. et al., Acetylated hsp70 and KAP1-mediated Vps34 SUMOylation is required for autophagosome creation in autophagy. *Proc. Natl. Acad. Sci. USA* 2013, *110*, 6841–6846.

[31] Caprioli, R. M., Farmer, T. B., Gile, J., Molecular imaging of biological samples: localization of peptides and proteins using MALDI-TOF MS. *Anal. Chem.* 1997, *69*, 4751–4760.

[32] Shamay, M., Liu, J., Li, R., Liao, G. et al., A protein array screen for Kaposi's sarcoma-associated herpesvirus LANA interactors links LANA to TIP60, PP2A activity, and telomere shortening. *J. Virol.* 2012, *86*, 5179–5191.

[33] Sun, R., Liang, D., Gao, Y., Lan, K., Kaposi's sarcoma-associated herpesvirus-encoded LANA interacts with host KAP1 to facilitate establishment of viral latency. *J. Virol.* 2014, *88*, 7331–7344.

[34] Si, H., Verma, S. C., Robertson, E. S., Proteomic analysis of the Kaposi's sarcoma-associated herpesvirus terminal repeat element binding proteins. *J. Virol.* 2006, *80*, 9017–9030.

[35] Lim, C., Gwack, Y., Hwang, S., Kim, S., Choe, J., The transcriptional activity of cAMP response element-binding protein-binding protein is modulated by the latency associated nuclear antigen of Kaposi's sarcoma-associated herpesvirus. *J. Biol. Chem.* 2001, *276*, 31016–31022.

[36] Krithivas, A., Young, D. B., Liao, G., Greene, D., Hayward, S. D., Human herpesvirus 8 LANA interacts with proteins of the mSin3 corepressor complex and negatively regulates Epstein-Barr virus gene expression in dually infected PEL cells. *J. Virol.* 2000, *74*, 9637–9645.

